

Critical dynamics of singlet excitations in a frustrated spin system

Valeri N. Kotov¹, Michael E. Zhitomirsky², and Oleg P. Sushkov^{2,3}

¹ Department of Physics, University of Florida, Gainesville, FL 32611-8440, USA

²Institute for Theoretical Physics, ETH-Hönggerberg, CH-8093 Zürich, Switzerland

³School of Physics, University of New South Wales, Sydney 2052, Australia

We construct and analyze a frustrated quantum spin model with plaquette order, in which the low-energy dynamics is controlled by spin singlets. At a critical value of frustration the singlet spectrum becomes gapless, indicating a quantum transition to a phase with dimer order. The magnetic susceptibility has an activated form throughout the phase diagram, whereas the specific heat exhibits a rich structure and a power law dependence on temperature at the quantum critical point. This generic behavior can be relevant to quantum antiferromagnets on Kagomé and pyrochlore lattices where (almost) all low-energy excitations are spin singlets, as well as to the CaV₄O₉ lattice.

PACS: 75.10.Jm, 75.30.Kz, 75.40.Gb, 75.40.-s

It was argued by Haldane and Chakravarty, Halperin and Nelson [1] that a quantum phase transition between a Néel state and a magnetically disordered phase in a two-dimensional (2D) quantum antiferromagnet is described by the 2+1 dimensional non-linear $O(3)$ σ -model. More recently the problem was studied in detail using the 1/N expansion [2] ($N = 3$ is the number of components of the order parameter), numerical methods [3] as well as the Brueckner method [4,5]. In this description the lowest quasiparticle excitation is a spin triplet. There are cases when a low-energy singlet excitation also appears, however it turns out to be irrelevant to the critical dynamics because of its vanishing spectral weight at the quantum critical point [6].

There is no doubt that the above picture based on triplet excitations describes a wide class of quantum phase transitions. On the other hand in Cr-based S=3/2 Kagomé materials it was found that at low temperatures ($T \lesssim 3 - 5$ K) the specific heat $C \propto T^2$ and is practically independent of magnetic field up to 12 T [7]. If we try to understand these data in terms of quasiparticles, the temperature behavior indicates a linear dependence of the excitation energy on momentum, and the insensitivity to field suggests that the quasiparticle spin is zero. Finite cluster numerical simulations for the S=1/2 Kagomé model indeed show that the lowest excitations are spin singlets with very small or zero gap [8]. Similar behavior with many singlet states inside the triplet gap was also found in the pyrochlore antiferromagnet [9] and the CaV₄O₉ lattice [10]. In the Kagomé case the singlet quasiparticle picture is far from being certain. It is unclear how to explain in this scenario the rather large zero temperature magnetic susceptibility observed in the Kagomé materials [7]. It is also possible that the material is a spin glass and hence a description in terms of quasiparticles would not be adequate. Nevertheless, it is very important and interesting to analyze the quasiparticle scenario. From this point of view the Kagomé magnets are critical (or close to critical) systems, and they certainly can not be described by the $O(3)$ σ -model. In the

present work we consider a two-dimensional spin system which exhibits a non-trivial singlet dynamics leading to a quantum critical point controlled by singlet excitations.

Critical singlet dynamics naturally appears in a spin model which has a zero temperature quantum phase transition between two singlet ground states. Both states are magnetically disordered but have different discrete lattice symmetries. We show that a spin model constructed as an array of weakly coupled frustrated plaquettes has only singlet low-energy degrees of freedom in a certain range of parameters. Many theoretical works have been devoted to the conventional order-disorder quantum phase transition in similar models, mainly in relation to the CaV₄O₉ compound [11–13]. A somewhat similar problem arises for the quantum dimer model [14], the Heisenberg model on a 3D pyrochlore lattice [15], and the generalized J_1 – J_2 model [16]. However, low-energy critical singlet dynamics for these systems has not been studied.

Consider a cluster of four S=1/2 spins (plaquette, see Fig.1(a)):

$$\hat{\mathcal{H}}_0 = J_1 \sum_{\langle ij \rangle} \mathbf{S}_i \cdot \mathbf{S}_j + J_2 \sum_{(ij)} \mathbf{S}_i \cdot \mathbf{S}_j, \quad (1)$$

where $\langle ij \rangle$ and (ij) denote, respectively, the side and diagonal bonds. We choose the diagonal coupling J_2 to be close to the side one: $J_2 \approx J_1 = J > 0$, and define $\alpha = J_1 - J_2 \ll J$. In this regime the spectrum of a plaquette is the following: two close singlet states which we denote by $|s_A\rangle$ and $|s_B\rangle$, with energy difference $\epsilon_B - \epsilon_A = 2\alpha$, three almost degenerate triplet states with excitation energy J above the singlets, and one S=2 state with energy $3J$. The two singlet wave functions are represented in terms of columnar dimer states as: $|s_A\rangle = \frac{1}{\sqrt{3}}\{|1, 2][3, 4] + |2, 3][4, 1]\}$ and $|s_B\rangle = \{|1, 2][3, 4] - |2, 3][4, 1|\}$, where $[i, j]$ denotes a singlet formed by the nearest-neighbor spins i and j (Fig.1(a)). Both singlets $|s_A\rangle$ and $|s_B\rangle$ are invariant under a four-fold rotation of a plaquette, whereas the columnar dimer states, e.g. $|1, 2][3, 4]$, break this symmetry. Consider now two decoupled plaquettes which for $\alpha = 0$

would have a 2×2 degenerate ground state. This degeneracy is lifted if we switch on a weak interaction between the plaquettes thus selecting one of the columnar dimer states. Such degeneracy lifting is different from the effect of a non-zero α , which leads to a nontrivial singlet dynamics in an array of weakly coupled plaquettes.

To be specific consider a square array with antiferromagnetic couplings j_1 between nearest-neighbor spins and j_2 between next-nearest-neighbor (diagonal) spins from different plaquettes, see Fig.1(b). For $j_1 = J_1$ and $j_2 = J_2$ it would be equivalent to the translationally-invariant 2D $J_1 - J_2$ model. However now we are interested in the weak-coupling limit: $j_1, j_2 \ll J_2 \approx J_1 = J$. The low-energy singlet sector of the Hilbert space has a natural pseudospin representation in terms of the states $|\uparrow\rangle = |s_A\rangle$ and $|\downarrow\rangle = |s_B\rangle$. The total Heisenberg spin Hamiltonian of the array of coupled plaquettes is mapped on the following pseudospin Hamiltonian to lowest order in the small parameters α and $j_{1,2}/J$:

$$\hat{\mathcal{H}} = -\Omega \sum_{\langle i,j \rangle} \left[\frac{1}{6} S_i^z S_j^z + \frac{1}{2} S_i^x S_j^x + \frac{e^{i\mathbf{Q}^{(i-j)}}}{2\sqrt{3}} (S_i^z S_j^x + S_i^x S_j^z) \right] - \Omega h \sum_i S_i^z. \quad (2)$$

The energy scale $\Omega = (j_1^2 + j_2^2)/2J$, and the effective dimensionless “magnetic field” is given by $h = [2\alpha + (j_1^2 + j_2^2 - 6j_1j_2)/6J]/\Omega$. We have also defined $\mathbf{Q} = (0, \pi)$ and dropped a constant term. The first sum in Eq.(2) is over nearest-neighbor plaquettes since bonds connecting second neighbors contribute only by a constant and thus do not change the singlet dynamics. We stress that (2) is an exact mapping of the original Heisenberg model in the low-energy sector (excitation energy $\omega \sim \Omega, \alpha \ll J$). The Hamiltonian $\hat{\mathcal{H}}$ describes an anisotropic ferromagnet in an external field. The interaction between pseudospins on adjacent sites is purely Ising, which can be seen by rotating the spin axes. However the Ising axis is staggered in the x - z plane deviating by angle $\pm\pi/6$ from the x -direction for horizontal (vertical) pairs.

The form of the Hamiltonian Eq.(2) is unaffected by asymmetry in the coupling constants j_1 and j_2 , which would only change the position of the reference zero-field level. In fact, the pseudospin Hamiltonian remains the same with parameters given by: $\Omega = j_1^2/2$ and $h = [2\alpha + (j_1^2 - 3j_1j_2)/6J]/\Omega$, even if we switch off one of the diagonal j_2 -bonds between nearest-neighbor plaquettes. In this case our model resembles the frustrated $\frac{1}{5}$ -depleted square lattice of CaV_4O_9 [11–13], which has next-nearest-neighbor couplings comparable or even exceeding the nearest-neighbor exchange. Thus our results apply to the singlet ground states of this magnet as well.

In zero “magnetic field” $h = 0$ the ground state of $\hat{\mathcal{H}}$ has broken Ising symmetry with all spins parallel or antiparallel to the \hat{x} direction. In the language of spin singlets breaking of Z_2 symmetry corresponds to sponta-

neous dimerization in one of the two columnar patterns. The rotational symmetry of the square lattice is obviously broken. The “magnetic field” tends to orient all spins along the \hat{z} axis, and depending on the sign of h favors either $|s_A\rangle$ or $|s_B\rangle$. Hence there are two critical fields, a positive and a negative one, for transitions into states with restored Z_2 symmetry. Since Eq.(2) is invariant under $h \rightarrow -h$, we consider the case $h > 0$ only.

To study in more detail the properties of the symmetric phase near the critical point we map the pseudospin Hamiltonian (2) onto a hard-core boson model. Positive and large h corresponds to $J_1 > J_2$. In this case we choose the bare ground state as $|0\rangle = \prod_i |s_A\rangle_i$. A boson creation operator on site i is defined by $|s_B\rangle_i = b_i^\dagger |s_A\rangle_i$. In terms of pseudospins we have $S_i^z = \frac{1}{2} - b_i^\dagger b_i$, $S_i^- = b_i^\dagger$. The resulting boson Hamiltonian is:

$$H_B = \epsilon \sum_i b_i^\dagger b_i + t \sum_{\langle ij \rangle} (b_i^\dagger b_j + b_i^\dagger b_j^\dagger + h.c.) + g \sum_{\langle ij \rangle} \pm (b_i^\dagger b_j^\dagger b_i + b_i^\dagger b_j^\dagger b_j + h.c.) + V \sum_{\langle ij \rangle} b_i^\dagger b_j^\dagger b_j b_i. \quad (3)$$

In the g -term the sign $+$ corresponds to a horizontal link and the sign $-$ to a vertical one. The parameters are:

$$\epsilon = \Omega(\frac{1}{3} + h), \quad t = -\frac{\Omega}{8}, \quad g = -\frac{\Omega}{4\sqrt{3}}, \quad V = -\frac{\Omega}{6}. \quad (4)$$

Considered in combination with the hard-core constraint $(b_i^\dagger)^2 = 0$, the Hamiltonian (3) is equivalent to the pseudospin Hamiltonian (2) and hence it is an exact mapping of the original spin problem in its low-energy sector.

The bosonic form of the effective Hamiltonian is convenient for the analysis of the low density (disordered) phase. Diagonalization of Eq.(3) in the quadratic approximation gives the following excitation spectrum: $\omega_{\mathbf{k}} = \sqrt{(\epsilon + 4t\gamma_{\mathbf{k}})^2 - (4t\gamma_{\mathbf{k}})^2}$, where $\gamma_{\mathbf{k}} = \frac{1}{2}(\cos k_x + \cos k_y)$. We set the inter-plaquette lattice spacing to one. The excitation gap $\Delta = \omega_{\mathbf{k}=0}$ vanishes at the critical point $h_c = \frac{2}{3}$. The other critical point is at $-h_c$. For $h > h_c$ the model is in the A-type plaquette phase, for $h < -h_c$ it is in the B-type plaquette phase, and in between $-h_c < h < h_c$ there is a phase with a boson condensate at $\mathbf{k} = 0$. The condensate is doubly degenerate because the boson field can have both signs.

The zero-point quantum fluctuations, which exist in the disordered (plaquette) phases, change slightly the critical field h_c . The simplest way to account for the correlation effects is to use the Brueckner technique developed in Ref. [4]. The cubic and quartic interactions in (3) are treated in the one-loop approximation, and the hard-core constraint is enforced via an infinite repulsion term $U \sum_i b_i^\dagger b_i^\dagger b_i b_i$, $U \rightarrow \infty$, added to the Hamiltonian (3). This interaction is taken into account in the Brueckner (low-density gas) approximation. The singlet gap obtained from the self-consistent solution of the resulting Dyson equations is plotted in Fig.2. At the critical

point the small parameter which justifies the Brueckner approximation is the singlet density $\langle b_i^\dagger b_i \rangle \approx 0.04$. The renormalized critical value $h_c \approx 0.65$ is only slightly below the result for non-interacting magnons. The reason is the strong compensation of the hard-core corrections by the one-loop diagrams arising from the cubic terms in Eq.(3). The dependence of the gap on h near the transition point agrees with the critical index $\nu = 0.63$, expected for the $O(N=1)$ σ model [17] and is quite different from the value $\nu = 0.5$ for non-interacting magnons.

Next we analyze the singlet excitation spectrum in the ordered dimer phase, $h < h_c$. We return to the pseudospin representation (2) and use the analogy between the evolution of the dimer phase and the spin reorientation process in an external magnetic field. The Holstein-Primakoff transformation is applied to the pseudospins in the rotating coordinate frame, which to lowest order coincides with the hard-core boson representation. At $h = 0$ all spins point along the \hat{x} -axis. For finite h the spins tilt towards the field direction at an angle $\sin \theta = h/h_c$. Keeping only quadratic terms we find the following “classical” spectrum of singlet excitations:

$$\omega_{\mathbf{k}} = \Omega \sqrt{1 - \gamma_{\mathbf{k}}(1 - \frac{2}{3} \cos^2 \theta) + \frac{1}{\sqrt{3}} \sin 2\theta \gamma_{\mathbf{k}+\mathbf{Q}}} . \quad (5)$$

In accordance with the broken discrete symmetry the singlet excitations have a finite gap $\Delta = \omega_{\mathbf{k}=0} = \Omega \sqrt{2(1 - h^2/h_c^2)/3}$, plotted in Fig.2. The gap vanishes at the critical point. Proceeding further with the spin analogy we have also calculated the “spin reduction” for the ferromagnet (2). This parameter shows how far is the real ground state wave-function from the approximate mean-field ansatz. At $h = 0$ we find $\langle S \rangle \approx 0.498$, meaning that the effect of quantum fluctuations is extremely small and linear spin-wave theory is well justified. At the transition point $h = h_c$ the zero-point oscillations are larger $\langle S \rangle \approx 0.44$ but still small enough to justify Eq.(5).

The broken Z_2 symmetry in the ground state at $|h| < h_c$ leads to a finite temperature transition. The whole phase diagram of the system of coupled plaquettes in the h - T plane is shown schematically in Fig.3. The critical temperature can be estimated as $T_c(h=0) \simeq \Omega$ (1.14 Ω for a pure Ising case). The phase transition between the ordered dimer and the plaquette states belongs to the 2D Ising universality class, and we therefore expect a logarithmic singularity in the specific heat: $C \sim \ln |T - T_c(h)|$. Below T_c the excitations acquire a gap and C goes exponentially at low temperatures. The same activated dependence holds also for the symmetric phases at $|h| > h_c$. However, when we approach the quantum critical points at $h = \pm h_c$ the gap becomes smaller and the low- T behavior of the specific heat changes to the quantum critical law $C_V = \gamma T^2$. The universal prefactor γ can be calculated using the Brueckner technique [5]. The result is $\gamma = \frac{12\zeta(3)}{5\pi c^2} \approx 0.92/c^2$, per plaquette, where $c = \Omega/2$ is the singlet excitation velocity at the

critical point (we set $k_B = \hbar = 1$). This value coincides with the large- N mean-field result [2]. Notice that, unlike C_V , the magnetic susceptibility is always activated $\chi \sim \exp(-\Delta_t/T), T \rightarrow 0$, since it is governed by the triplet gap $\Delta_t \sim J$.

The variation of C_V as a function of temperature is schematically presented in Fig.4 for the different parts of the phase diagram. In addition to the singlet contribution, whose form was discussed above, we have also shown the peaks arising from the higher energy triplet and quintuplet states. We estimate that the singlets contribute about 25% to the entropy $S = \int (C_V/T) dT$ (and 61% and 14% are taken by the S=1 and S=2 states, respectively). The possibility of rich behavior at low T has been debated for some time for the Kagomé antiferromagnet and a sharp structure is believed to exist due to low-energy singlets [18]. Notice that in our model a very peculiar behavior with a logarithmic singularity sets in at $h < h_c$ which crosses over to the quantum critical regime at $h = h_c$. Such a sharp feature is generic for systems near a transition between two singlet ground states.

In conclusion we have analyzed a quantum spin model with purely singlet low-energy dynamics. There is a quantum phase transition in the model separating a disordered plaquette phase and a columnar dimer phase. Even though the inter-plaquette interaction was assumed to be weak, we expect our results to hold also for stronger interactions as long as there are no other instabilities, and to be applicable, e.g. to CaV_4O_9 . The broken symmetries in the singlet ground state of CaV_4O_9 were considered previously in Ref. [12] in the framework of the quantum dimer model. However the columnar dimer ordering found in the present work never corresponds to the ground state in [12], which possibly indicates a weakness of the dimer model applied to a real spin system with Heisenberg interactions.

We have found that while the magnetic susceptibility is always activated, the specific heat behavior is very rich and changes substantially in the different regimes. The model was inspired by experimental and numerical data for Kagomé systems and also shares common structure with pyrochlore antiferromagnets and CaV_4O_9 . The novel quantum critical behavior associated with singlet criticality discussed in this work can be relevant to a wide class of disordered quantum spin systems.

We are grateful to C. Lhuillier, F. Mila, A.P. Ramirez, R.R.P. Singh, and W.H. Zheng for stimulating discussions. This work was supported by NSF Grant DMR9357474 (V.N.K.), in part by NSF Grant PHY94-07194 (O.P.S.), and by the Swiss National Fund (M.E.Z.).

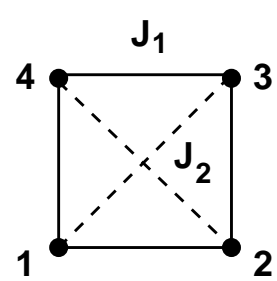
- [1] F.D.M. Haldane, Phys. Rev. Lett. **50**, 1153 (1983); S. Chakravarty, B.I. Halperin, and D.R. Nelson, Phys. Rev. B **39**, 2344 (1989).
- [2] A.V. Chubukov, S. Sachdev, and J. Ye, Phys. Rev. B **49**, 11919 (1994).
- [3] A.W. Sandvik and D.J. Scalapino, Phys. Rev. Lett. **72**, 2777 (1994); W.H. Zheng, Phys. Rev. B **55**, 12267 (1997).
- [4] V.N. Kotov *et al.*, Phys. Rev. Lett. **80**, 5790 (1998).
- [5] P.V. Shevchenko, A.W. Sandvik, and O.P. Sushkov, cond-mat/9905227.
- [6] V.N. Kotov and O.P. Sushkov, cond-mat/9907178.
- [7] A.P. Ramirez, G.P. Espinosa, and A.S. Cooper, Phys. Rev. Lett. **64**, 2070 (1990); A.P. Ramirez, private communication.
- [8] C. Waldtmann *et al.*, Eur. Phys. J. B **2**, 501 (1998).
- [9] B. Canals and C. Lacroix, Phys. Rev. Lett. **80**, 2933 (1998).
- [10] M. Albrecht, F. Mila, and D. Poilblanc, Phys. Rev. B **54**, 15856 (1996).
- [11] K. Ueda *et al.*, Phys. Rev. Lett. **76**, 1932 (1996); O.A. Starykh *et al.*, *ibid.* **77**, 2558 (1996).
- [12] S. Sachdev and N. Read, Phys. Rev. Lett. **77**, 4800 (1996).
- [13] W.H. Zheng *et al.*, Phys. Rev. B **55**, 11377 (1997).
- [14] D. Rokhsar and S. Kivelson, Phys. Rev. Lett. **61**, 2376 (1988); P.W. Leung, K.C. Chiu and K.J. Runge, Phys. Rev. B **54**, 12938 (1996).
- [15] A.B. Harris, A.J. Berlinsky and C. Bruder, J. Appl. Phys. **69**, 5200 (1991).
- [16] R.R.P. Singh *et al.*, Phys. Rev. B **60**, 7278 (1999).
- [17] R. Guida and J. Zinn-Justin, J. Phys. A **31**, 8103 (1998).
- [18] P. Sindzingre *et al.*, cond-mat/9907220.

FIG. 1. (a) A single frustrated plaquette. (b) An array of interacting plaquettes.

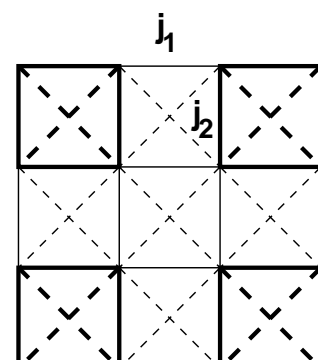
FIG. 2. Singlet gap in the vicinity of the quantum critical point separating the plaquette and dimerized phases.

FIG. 3. Schematic phase diagram of the model. The solid line represents the 2D Ising critical line, and the dots are the two quantum critical points belonging to the $O(1)$ (equivalently 3D Ising) universality class.

FIG. 4. Temperature dependence of the specific heat throughout the plaquette phase, $h > h_c$, down to the quantum critical point $h = \pm h_c$ (top), as well as for $h < h_c$, across the 2D Ising critical line (bottom).



(a)



(b)

Fig.1.

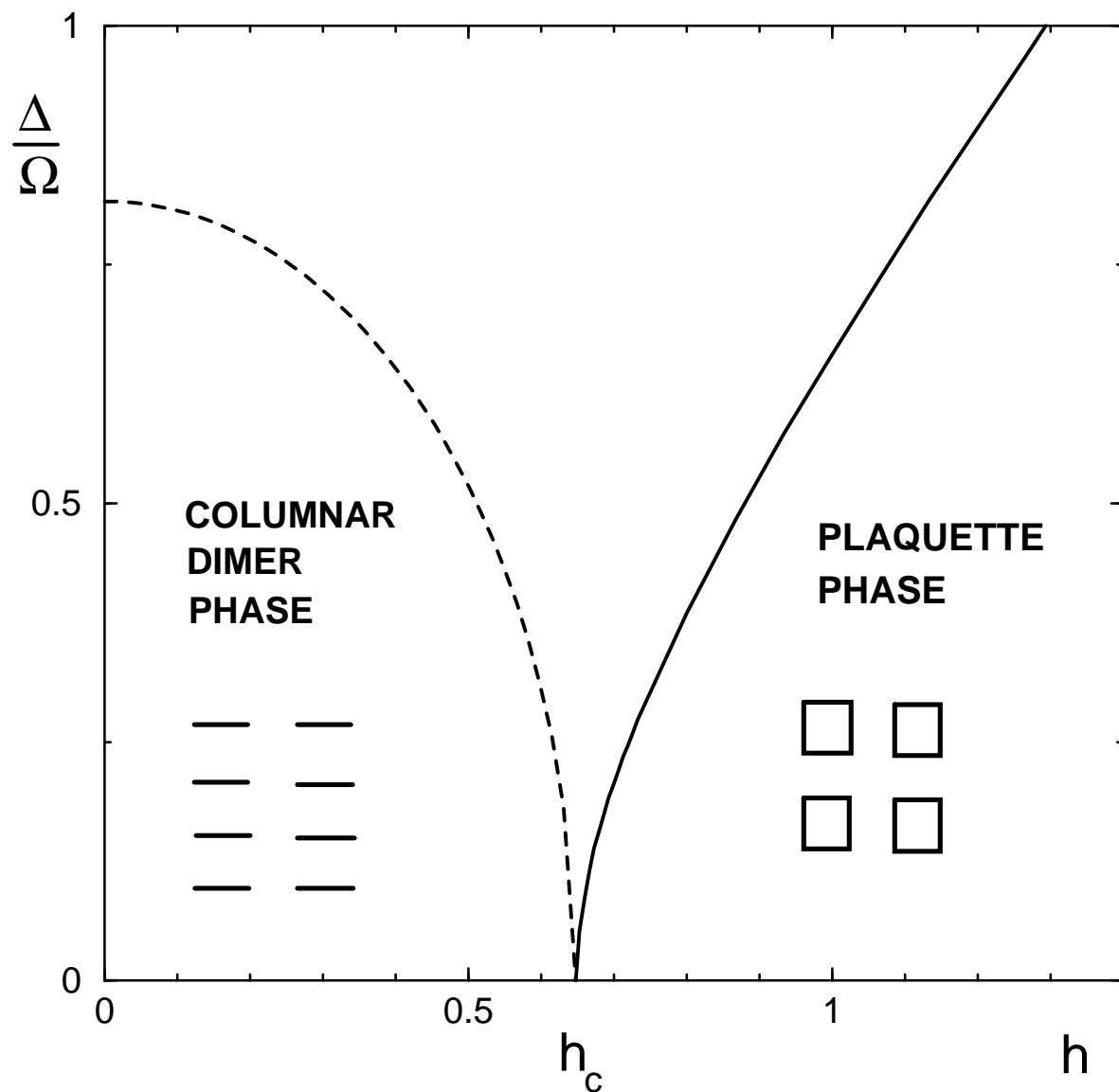


FIG.2.

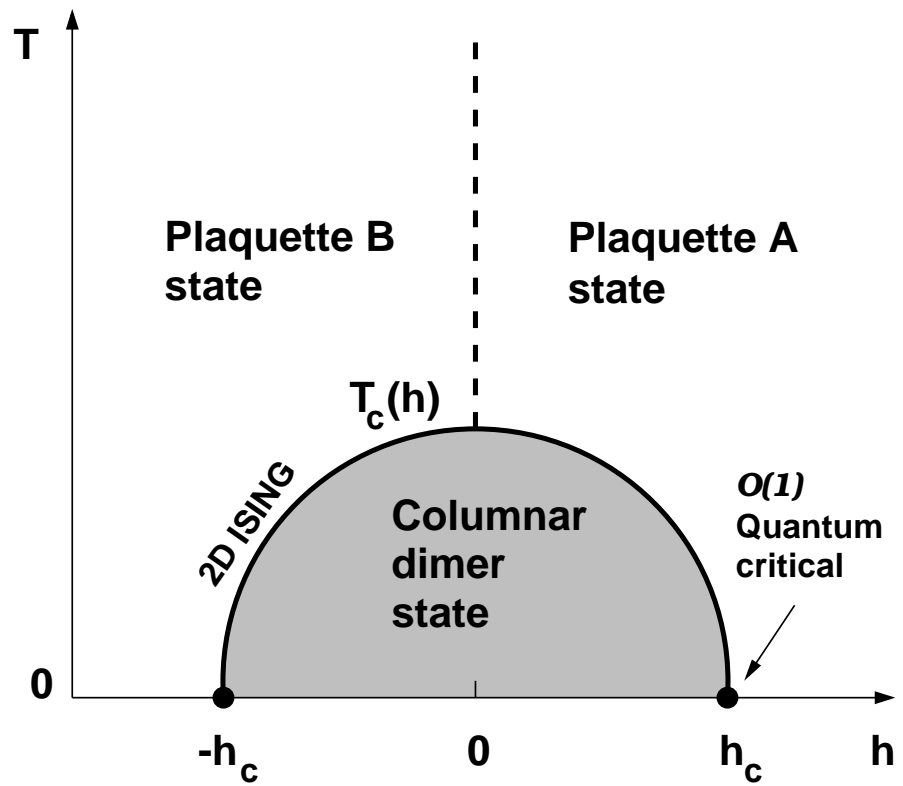


FIG.3.

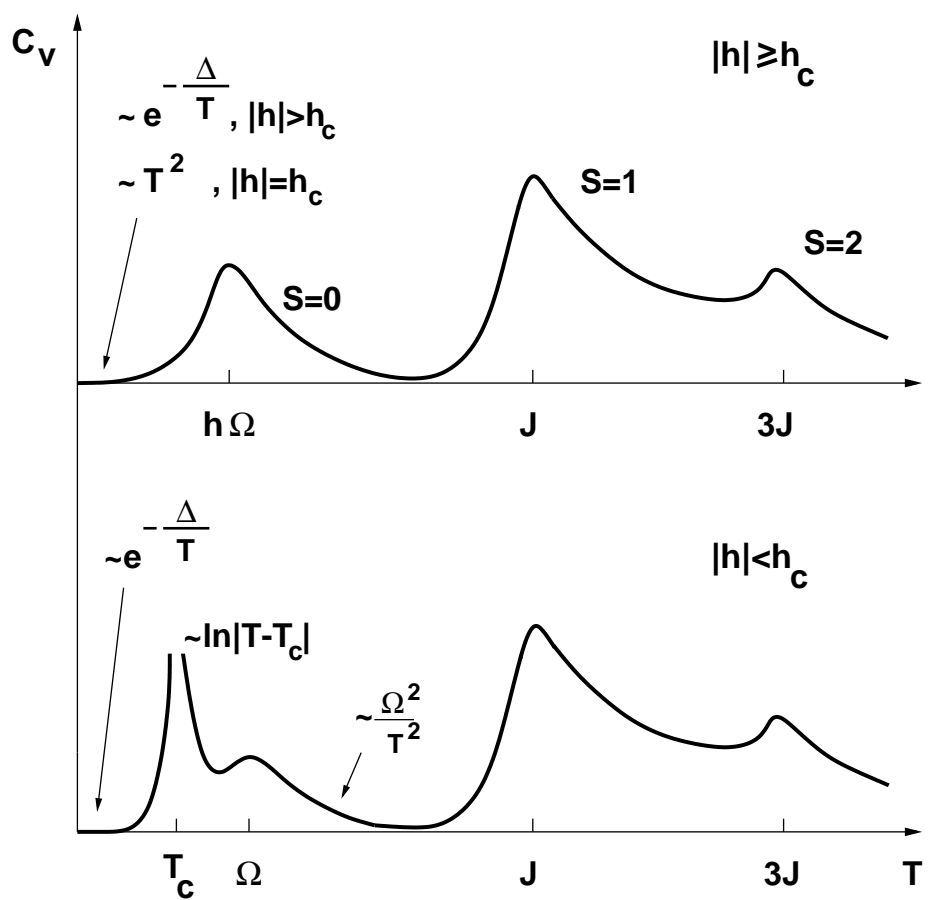


FIG.4.